

Suggestion of Potential Stent Design Parameters to Reduce Restenosis Risk driven by Foreshortening or Dogboning due to Non-uniform Balloon-Stent Expansion

DOHYUNG LIM,^{1,2} SEUNG-KWAN CHO,^{1,2} WON-PIL PARK,^{1,2} ANDERS KRISTENSSON,³ JAI-YOUNG KO,⁴
S. T. S. AL-HASSANI,³ and HAN-SUNG KIM^{1,2}

¹Department of Biomedical Engineering, Yonsei University, Wonju, Kangwondo, Republic of Korea; ²Research Institute for Medical Instruments & Rehabilitation Engineering, Yonsei University, 234, Maeji-Ri, Heungup-Myun, Wonju, Kangwondo 220-710, Republic of Korea; ³Department of Mechanical, Aerospace & Manufacturing Engineering, University of Manchester, Manchester, UK; and ⁴M.I. Tech Co., Ltd. Seoul, Seoul, Republic of Korea

(Received 7 August 2007; accepted 10 April 2008; published online 24 April 2008)

Abstract—The foreshortening or dogboning of a stent that occurs due to transient non-uniform balloon-stent expansion can induce a vascular injury, resulting in restenosis of the coronary artery. However, previous studies rarely considered the effects of transient non-uniform balloon expansion on analysis of the mechanical properties and behaviors of stents during stent deployment, nor did they determine design parameters to minimize the restenosis risk driven by foreshortening or dogboning. The aim of the current study was, therefore, to suggest potential design parameters capable of reducing the possibility of restenosis risk driven by foreshortening or dogboning through a comparative study of seven commercial stents using finite element (FE) analyses of a realistic transient non-uniform balloon-stent expansion process. The results indicate that using stents composed of opened unit cells connected by bend-shaped link structures, in particular the MAC Plus stent, and controlling the geometrical and morphological features of the unit cell strut or the link structure at the distal ends of stent may prevent restenosis risk caused by foreshortening or dogboning. This study provides a first look at the realistic transient non-uniform balloon-stent expansion by investigating the mechanical properties, behaviors, and design parameters capable of reducing the possibility of restenosis risk induced by the foreshortening or the dogboning.

Keywords—Stent, Foreshortening, Dogboning, Transient non-uniform balloon expansion, Finite element analysis.

ABBREVIATIONS

FE	Finite element
C3D8R	Eight-node linear brick solid elements
S4R	Four-node shell elements

F3D4	Four-node hydrostatic fluid elements
POI	Point of interest
E	Elastic modulus (Y_s)
Y_s	Yield stress
ν	Poisson ratio
r_1	Outer radius of the balloon
r_2	Middle radius of the balloon
r_3	Inner radius of the balloon
r_s	Initial inner radius of the stents
d_1	Length of the first membrane of the balloon
d_2	Length of the second membrane of the balloon
d_3	Length of the third membrane of the balloon
d_f	Target balloon diameter
L	Initial length of the stent
L^{load}	Longitudinal length of the stent
$R^{\text{load}}_{\text{central}}$	Central radius of the stent
$R^{\text{load}}_{\text{POI}}$	Radius at point of interest of the stent

INTRODUCTION

In the United States, cardiovascular diseases are one of the principal causes of mortality, with a socio-economic burden estimated to reach \$400 billion dollars in 2006.³² Atherosclerosis, also known as coronary artery disease, is one of the most serious forms of cardiovascular disease that affects the arterial blood vessel.^{6,32} It is characterized by a chronic inflammatory response in the walls of arteries, in large part due to the deposition of lipoproteins (atheromatous plaques known as plasma proteins that carry cholesterol and triglycerides). This leads to a thickening of the artery

Address correspondence to Han-Sung Kim, Research Institute for Medical Instruments & Rehabilitation Engineering, Yonsei University, 234, Maeji-Ri, Heungup-Myun, Wonju, Kangwondo 220-710, Republic of Korea. Electronic mail: hanskim@yonsei.ac.kr

walls, resulting in a reduction of blood flow by narrowing or even blocking (restenosis) the arteries.

Currently, three of the most common treatments for a coronary artery disease that does not respond to pharmacologic therapy are coronary artery bypass grafting, percutaneous transluminal coronary balloon angioplasty, and percutaneous transluminal coronary stenting with the aid of coronary balloon angioplasty. Of these, at present, the vascular intervention market for coronary stents has increased rapidly because of their high initial success rate, minimal invasive nature, and improved long-term effectiveness compared to coronary artery bypass grafting or percutaneous transluminal coronary balloon angioplasty.^{14,29,33} Each year, over 1 million percutaneous interventions are performed worldwide, exceeding the annual number of coronary artery bypass grafts. The use of coronary stents in interventional procedures has rapidly increased from 10% in 1994 to over 80% in current practice.^{17,33} In a recent review of randomized trials comparing the stenting technique with balloon angioplasty, the stenting technique reduced the rates of repeat revascularization by 35–75%, while angiographic indexes of the restenosis were decreased by 20–55%.^{17,31}

Stent generally features either an expandable wire or perforated tube that is inserted into an artery to prevent or counteract a disease-induced localized blood flow constriction. The first stent was introduced and implanted by Dotter¹⁰ to treat arterial shrinkage. Clinical utilization of stents has been widely accepted in the 1990s to improve the limitations of balloon angioplasty, such as restenosis and abrupt closures of the arteries.^{9,21} However, potential limitations, such as restenosis,^{12,14,29} migrations,^{15,34} collapses,^{3,27} or positioning difficulties,¹⁹ are still seen in clinical utilization of stents. Among these potential limitations, restenosis has become the main bottleneck to the development of stenting techniques.^{30,33} There are several mechanisms that lead to restenosis. The most important is the inflammatory response, which induces a tissue proliferation (neointimal hyperplasia) around the angioplasty site.^{18,28} Kastrati *et al.*¹⁸ showed that the incidence of restenosis ranged from 20 to 50%, depending on the stent design, in a clinical study of 4510 stent placements. Issues with respect to the design of coronary artery stents generally include: (1) radial stiffness, (2) flexibility, (3) minimal foreshortening (contraction in length of the stent as dilating the stent), (4) minimal dogboning (larger expansion in diameter at the distal point compared with that at the central point of the stent as dilating the stent: flaring of stent ends), (5) minimal longitudinal recoil, (6) minimal radial recoil, (7) minimal coverage area, and (8) fatigue durability.^{13,33} These issues are related directly or indirectly to restenosis.

It is widely accepted that finite element (FE) analysis is powerful tools for rapid investigation and improvement of design concepts prior to clinical trials. Rogers *et al.*²⁶ studied a two-dimensional balloon–artery interaction during stent placement. Dumoulin and Cochelin¹¹ evaluated and characterized the mechanical properties and behaviors of a balloon expandable stent. Etave *et al.*¹³ compared the performance of two types of stents. Berry *et al.*² assessed the hemodynamics and wall mechanics of compliance matching stents in a stent–artery hybrid structure. Chau *et al.*^{5–8} investigated stent expansion, balloon–stent interaction, expansion characteristics of slotted tube stents in the presence of plaques and arteries, and the effect of varying the slotted tube stent geometry on its expansion behavior. Migliavacca *et al.*^{21–23} assessed the mechanical properties and behavior of balloon-expandable stents to determine how the FE method could be used to optimize stent designs. They also compared the performance of stainless steel stents with shape memory alloy stents by analyzing the stress on the vascular wall induced by the expansion of balloon- and self-expandable stents, and demonstrated how the mechanical properties and behaviors of new generation balloon-expandable stents could be studied accurately with computational analyses based on the FE method. Wang *et al.*³³ investigated the transient expansion behavior of six models of balloon-expandable stents and proposed a new modified stent based on their comparative study. Previous studies have not, however, investigated transient non-uniform balloon expansion during stent deployment. They thought that it seemed justifiable to model balloon expansion by considering uniform radial internal pressure. Such assumption was based on the fact that stent is almost uniformly dilated and finally evenly expanded. That was only true away from the ends of stent. Therefore, in order to fully understand the mechanical properties and behaviors of stent, it is necessary to consider a realistic modeling of transient non-uniform balloon-stent expansion with FE analysis. Particularly, considering the realistic transient non-uniform balloon-stent expansion is especially important because an undesirable foreshortening or dogboning driven during stent deployment can initiate vascular restenosis injuries. Thus, in study of the mechanical properties and behaviors of foreshortening or dogboning of stent, the realistic transient non-uniform balloon-stent expansion should be considered.

The aim of the current study is to suggest potential design parameters capable of reducing a risk of vascular restenosis injuries, which can be induced by foreshortening and dogboning, through a comparative study of recently developed seven commercial stents

using FE analyses of the realistic transient non-uniform balloon-stent expansion process.

MATERIALS AND METHODS

Stent FE Model

Three-dimensional FE models of seven commercial stents (Palmaz-Schatz PS153, TenaxTM, MAC Standard, MAC Q23, MAC Plus, Coroflex, RX Ultra

Multi-link) were created using Hypermesh 7.0 (Altair Engineering, Inc., USA) (Fig. 1) based on the manufacturers' specifications. The structural specifications of the stents are summarized in Table 1. The Palmaz-Schatz PS 153 stent (Johnson and Johnson Co., USA) was manufactured as a tubular structure composed of a closed rectangular unit cell without a link structure in the longitudinal direction of the stent (Fig. 1a). The TenaxTM stent (Biotronik, Germany) had a tubular structure composed of a closed unit cell with a

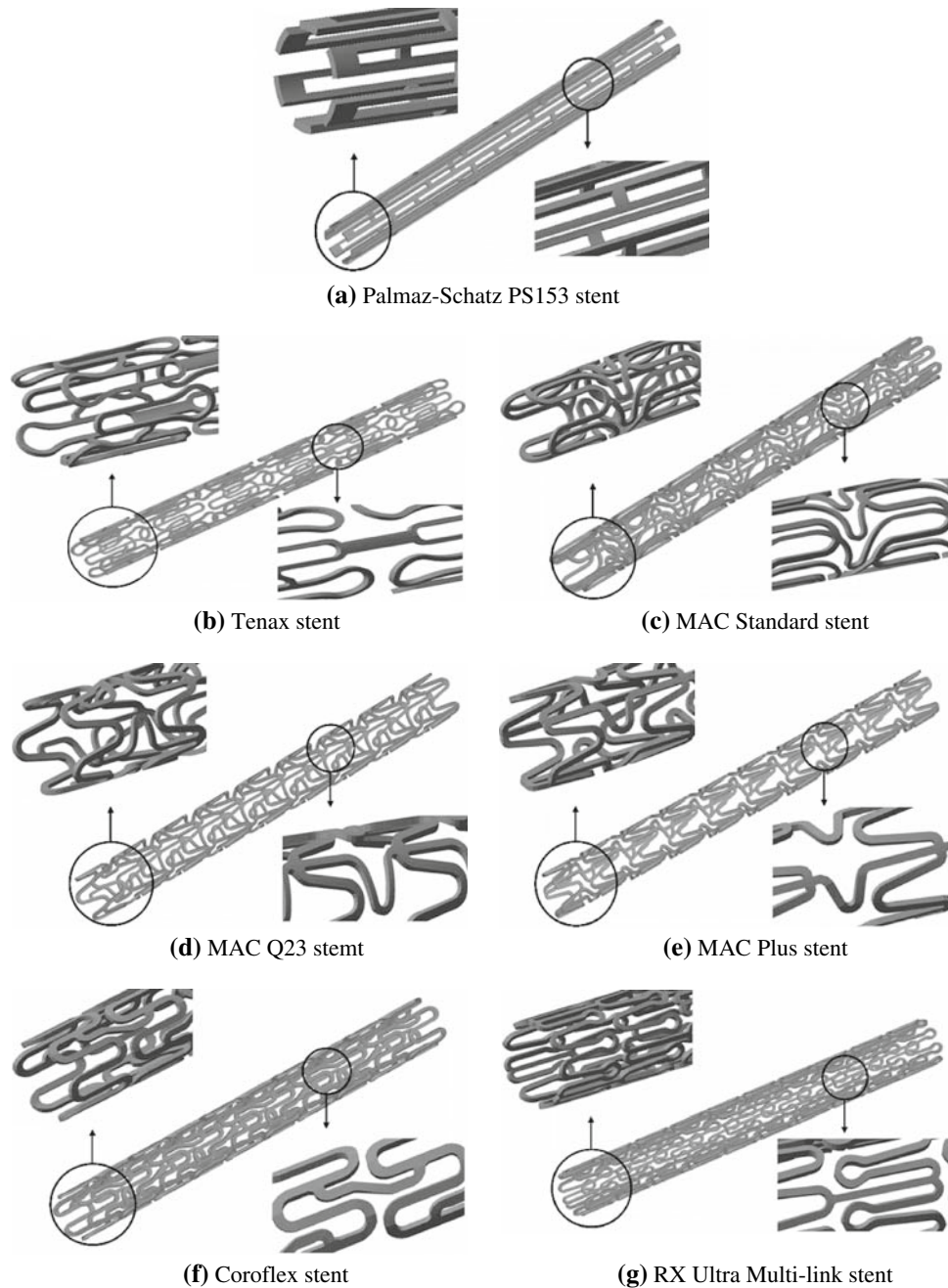


FIGURE 1. Final three-dimensional FE models of the seven commercial stents.

TABLE 1. Structural specifications of the seven commercial stents analyzed in the current study, determined based on the manufactures' specifications.

Stent/Item	General structural parameters for the stent				Unit cell structural parameters	Structural parameters in the link structure	
	Outer diameter (mm)	Inner diameter (mm)	Strut thickness (mm)	Length (mm)	Strut width (mm)	Strut width (mm)	Strut length (mm)
Palmaz-Schatz PS15	1.484	1.389	0.095	16.0	0.106	0.106	3.720
Tenax	1.780	1.695	0.085	15.1	0.083	0.199	0.834
MAC Standard	1.800	1.715	0.085	16.8	0.125	0.125	3.581
MAC Q23	1.800	1.715	0.085	16.8	0.126	0.100	2.764
MAC Plus	1.764	1.669	0.095	15.0	0.125	0.125	3.487
Coroflex	1.725	1.630	0.095	15.9	0.136	0.135	1.647
RX Ultra Multi-link	1.764	1.669	0.095	15.0	0.097	0.096	1.382

corrugated ring pattern and an independent bar link structure in the longitudinal direction of the stent (Fig. 1b). The MAC Standard stent (amg GmbH, Germany) had a tubular structure composed of an opened unit cell with a sinusoidal curvature and an independent link structure of a bend-shaped connector arranged asymmetrically in the longitudinal direction of the stent (Fig. 1c). The MAC Q23 and Plus stents (amg GmbH, Germany) and the Coroflex stent (B. Braun Melsunen AG, Germany) had a tubular structure composed of an opened unit cell with a sinusoidal curvature and an independent link structure of a bend-shaped connector arranged symmetrically in the longitudinal direction of the stent (Figs. 1d–f). The RX Ultra Multi-link stent (Guidant, USA) was composed of a tubular structure connected by an opened unit cell with a corrugated wave pattern and an independent straight-line link structure arranged in the longitudinal direction of the stent (Fig. 1g). The final FE models of the stents consisted of 16,320–27,584 eight-node linear brick solid elements (C3D8R). Here, two layers of elements were considered for representation of the strut thickness of the stent (Fig. 2d, right). One layer of the strut of the stents was therefore consisted of 8160–13,792 eight-node linear brick solid elements. To avoid inaccuracy of FE results due to improper mesh on the curved portion of the FE model, a great number of elements were incorporated into the curved portion compared with elements used for the straight portion of the strut of the stent. Here, the ratio of the elements incorporated into the curved to the straight portions was average 2–1.

Balloon-Catheter FE Model

The three-dimensional FE model of the stent balloon was also built using Hypermesh 7.0 based on the actual contours of the balloon (Fig. 2). During the initial phase of expansion, the balloon was represented by folding the membrane into a unit cell (hereafter

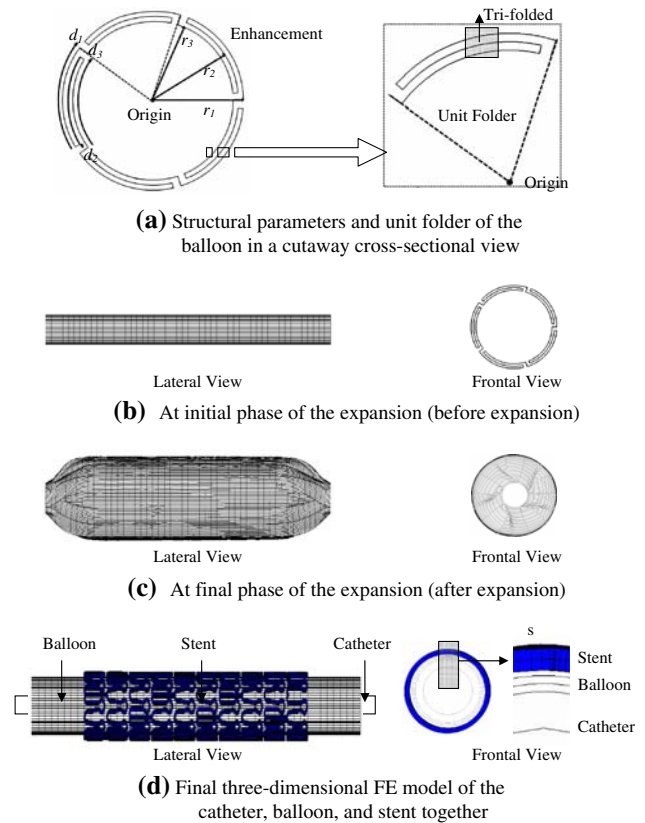


FIGURE 2. Final three-dimensional FE model of the balloon for the stent and its schematic diagram at a cutaway cross-sectional view used to illustrate the tri-folded membrane in the unit folder and the structural parameters of the balloon.

called the “unit folder”) as shown in Fig. 2a. Then, five unit folders were considered in a cutaway cross-sectional view. For each unit folder, the membrane was tri-folded, resulting in the formation of three layers, based on the fact that an actual balloon is usually tri-folded before being crimped onto the stent³³ and on the necessary and sufficient condition that the membrane must be unfolded completely at the final phase

of the expansion. The outer radius of the balloon (r_1 , from the first membrane layer to the center of the balloon), middle radius of the balloon (r_2 , from the second membrane layer to the center of the balloon), and inner radius of the balloon (r_3 , from the third membrane layer to the center of the balloon) were 0.62, 0.58, and 0.55 mm, respectively, and the lengths of the first (d_1), second (d_2), and third (d_3) membranes were 0.72, 0.63, and 0.64 mm, respectively. These yielded a target balloon diameter (d_f) of 3.00 mm at the final phase of the expansion, which is equal to a typical original artery diameter.^{21,33} Other structural parameters and their values considered in the current study are shown in Fig. 2. The final FE models of the balloon consisted of 10,700 four-node shell elements (S4R) and 10,700 four-node hydrostatic fluid elements (F3D4) (Fig. 2). A thickness of 0.033 mm measured from the actual membrane of the balloon was assigned to the shell elements. The hydrostatic fluid elements were used to simulate the balloon expansion by changing the amount of fluid in a fluid-filled cavity. This process will be explained in detail below.

The shaft in the catheter that allows fluid to be injected into the balloon was developed as a rigid body to establish a datum point for the balloon expansion (Fig. 2). The diameter of the shaft was matched to the caliber of the balloon, and the length of the shaft was slightly larger than that of the balloon (Fig. 2).

Constitutive Material Models

The stents were assumed to be made of 316L stainless steel, which had an elasto-plastic constitutive behavior obtained from an engineering stress–strain curve reported by Albertini and Montagnani.¹ The general mechanical properties of this material were 196 GPa for an elastic modulus (E), 308 MPa for a yield stress (Y_s), and 0.33 for a Poisson ratio (ν).¹

The balloon was assumed to be made of high-density polypropylene that had an isotropic linear elasticity. The mechanical properties of the material were then determined from literature (E : 1 GPa, Y_s : 90 MPa, and ν : 0.33).²⁰

Boundary and Contact Conditions

Two boundary conditions were assigned to the ends of the balloon and to the shaft of the catheter, and two contact conditions were used between the folded membranes of the balloon and between the stent and the balloon (Fig. 3). A pin joint boundary condition was used for the balloon based on the fact that the balloon generally expands to an ellipsoid form, as shown in Fig. 3. A fixed joint boundary condition was

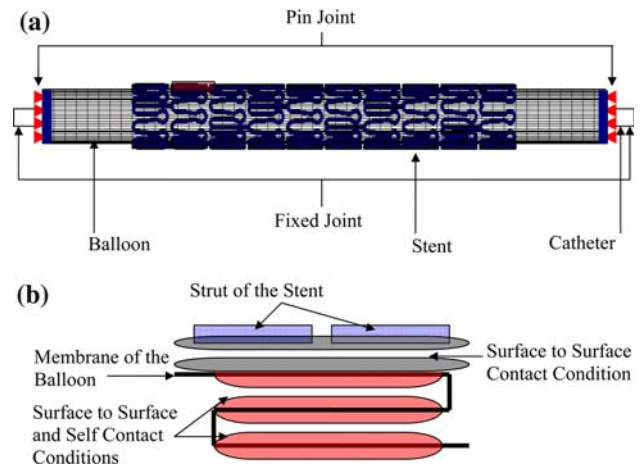


FIGURE 3. (a) Boundary and (b) contact conditions used in the current study. The lateral view of the contact region between the stent and the balloon was enlarged for clarity.

assigned to the rigid-body shaft of the catheter to avoid movement of the catheter in all directions during the balloon expansion. Surface-to-surface contact conditions were used between the stent and the balloon, while surface-to-surface and self-contact conditions were used for the folded membranes during the expansion of the balloon.

Simulation of the Transient Non-uniform Balloon-Stent Expansion

The transient non-uniform balloon simulation was performed in three steps. First, the simulation mimicked the free expansion of the stent until the initial radius ($r_1 = 0.62$ mm) of the balloon reached the value of the initial inner radius of the stents ($r_s = 0.65$ mm for the Palmaz-Schatz PS153 stent, 0.81 mm for the TenaxTM stent, 0.79 mm for the MAC Standard and Q23 stents, 0.82 mm for the MAC Plus stent, 0.77 mm for the Coroflex stent, and 0.82 mm for the RX Ultra Multi-link stent). Second, the simulation was used to examine dogboning to a diameter of 3 mm, corresponding to the typical inner diameter of a coronary artery.^{21,33} Finally, the simulation was used to investigate foreshortening after the balloon was removed. The stents were then unloaded, decreasing the internal pressure to zero. The definition of the mechanical properties and behavior will be explained in detail below.

The balloon-stent expansion was performed by controlling the features of the hydrostatic fluid elements. A pneumatic flow at 1 atm and surgical room temperature was used for the stent, with an amplitude option that allowed arbitrary time variations of the

amount of fluid mass (fluid mass flow rate) to be supplied throughout the simulation. A fluid flux option was used to specify changes in the fluid mass of the fluid-filled cavity modeled with the hydrostatic fluid elements. Thus the balloon-stent expansion was controlled by a change in the amount of fluid mass (volume controlled process).

The ABAQUS 6.3 package (ABAQUS, Inc., Providence, RI, USA) was used to solve the FE models. Both the explicit and implicit ABAQUS commercial codes were used for all steps.

Validation of the FE Simulations

Sensitivity (convergence) tests of the stent FE models were performed to identify the influence of the number of elements on the FE results. The number of elements for each stent FE model was 0.5 times decreased (coarsest mesh model) or 1.5 times increased (finest mesh model) gradually relative to the original mesh model (used in the current study), and the resulting foreshortening and dogboning values were examined and compared. Additional temporal sensitivity tests were also conducted by specifying explicit time integration for all stent FE models in the original mesh model. For this temporal sensitivity tests, time period of the step was altered from 130 to 170 at an interval of 10, and a degree of convergence of FE simulation for each time period and difference between the FE results obtained from the defined time periods were examined and compared with each other.

Validation of our FE simulations of stent-balloon expansions was performed by comparing our predicted expansion process, as well as the diameter and internal pressure at five points of interest (POIs) (Fig. 4) with experiment results analyzed from the literature.^{11,24,33}

Comparative Study

The evaluation of the stents focused on analyzing the mechanical properties and behaviors of foreshortening and dogboning, which could be influenced by the

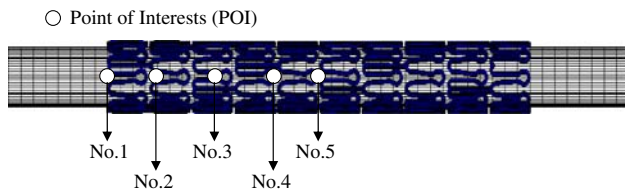


FIGURE 4. Five POIs used for to validate the FE simulation for the transient non-uniform balloon-stent expansion process. The relationship between the internal pressure and the diameter of the balloon-stent during the transient non-uniform balloon-stent expansion process was identified using the FE predictions at the POIs.

characteristics of the balloon-stent expansion, to identify potential design parameters that reduce restenosis induced by undesirable mechanical stress on the vascular wall.^{11,24,32,33} In general, the stent must be deployable to various locations in coronary arteries in a simple and safe manner, and be capable of expanding the wall of the artery.^{5,6,11,13,24,32,33} The stent must have a sufficiently high plastic ductility (indexed by flexibility or radial stiffness) and low elastic recoil (indexed by longitudinal or radial recoil).^{11,13,21,24,32} These mechanical requirements are of crucial importance and must be achieved by the specific design and material used for the stent to give a high tensile strength, yield strength, and ductile yield. However, the current study was focused on the mechanical properties and behaviors of foreshortening and dogboning.

The following equations^{24,33} were used to define foreshortening and dogboning:

$$\text{Foreshortening} = \frac{L - L^{\text{load}}}{L} \times 100\% \quad (1)$$

$$\text{Dogboning} = \frac{R_{\text{POI}}^{\text{load}} - R_{\text{central}}^{\text{load}}}{R_{\text{distal}}^{\text{load}}} \times 100\% \quad (2)$$

where L^{load} , $R_{\text{central}}^{\text{load}}$, and $R_{\text{POI}}^{\text{load}}$ are the longitudinal length, the central radius, and the radius at the POI of the stent, respectively, after the loading due to the stent-balloon expansion, and L is the initial length of the stent.

RESULTS

Accuracy of the FE Simulation

The sensitivity test identifying the influence of the number of elements on the FE simulation results showed that the percent differences in the results between the original mesh and the other meshes were generally within approximately 0.4% for the coarsest mesh and approximately 0.2% for the finest mesh. This fact indicates that it is possible to conclude that a number of elements are not sensitive to the grid refinement of the mesh. The additional temporal sensitivity test performed by specifying explicit time integration showed that the FE simulation was convergent over 150 time period and the differences between the FE simulation results obtained over 150 time period were within almost 0%. These facts indicate that it is possible to conclude that the FE results are not sensitive to the time period over 150. Based on these facts, the original mesh and the 160 time period were used for all FE simulations performed in the current study.

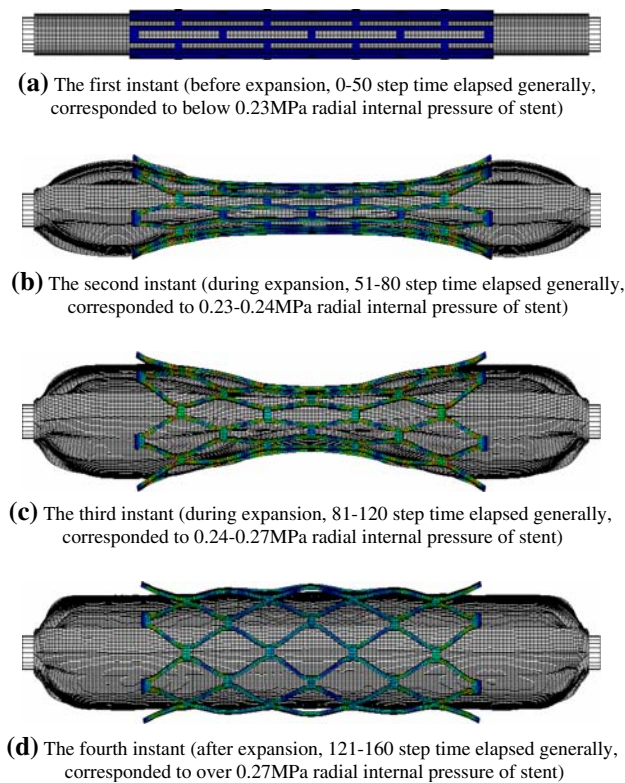


FIGURE 5. Pattern of the transient non-uniform balloon-stent expansion at four different instants during the expansion process. Only the expansion pattern for the Palmaz-Schatz PS153 stent is shown (a) before expansion, (b) and (c) during expansion, and (d) after expansion.

The pattern of the transient non-uniform balloon-stent expansion at four different instants during the expansion process is shown in Fig. 5. Only the expansion pattern for Palmaz-Schatz PS153 stent is shown because all stents had similar expansion patterns. The radial displacement (volume change) in the distal region of the stent was larger than the central displacement at the second and third instants shown in the figure. However, the radial displacement in the distal region of the stent was equal to the central displacement at the fourth instant shown in the figure, corresponding to the final phase of the expansion. These results compared favorably with those reported in the literature.^{11,24,33}

The pressure–diameter curves for the transient non-uniform balloon-stent expansion process are shown in Fig. 6 for the balloon-stents analyzed in the current study. Results from the literature are also shown.^{24,33} In the period from the time that fluid was supplied to the balloon to the time that the balloon was fitted closely to the stent (Phase 1 in Fig. 6), our FE results indicated that the balloon diameter of all the stents was rarely changed. In the next stage (Phase 2 in Fig. 6) our FE results for all balloon-stents indicated a large

increase in diameter with little increase in pressure, which corresponds to a burst-open or a chain-reaction deformation of the stent. This might indicate that the energy stored in the stent structure during the expansion of the stent was transformed into local plastic deformation so that the entire structure entered a state of plastic instability. Continuously, once all the weak parts of the stent had deformed plastically, further expansion required a high increase in pressure because of the limitation of the balloon expansion and the strain hardening of the stent material (Phase 3 in Fig. 6). The pressure–diameter curves predicted from our FE simulations for all balloon-stents compared favorably with those reported in the literature, as shown in Fig. 6.^{24,33}

Foreshortening and Dogboning of the Seven Commercial Stents

The foreshortening and dogboning results for the seven commercial stents are summarized in Table 2, and Figs. 7 and 8.

The foreshortenings, which depended on the geometrical and morphological characteristics of the stent, were ranged from 0.0% for the MAC Plus stent to 12.9% for the TenaxTM stent (Table 2 and Fig. 7). For all stents except to MAC Plus, the foreshortening was occurred abruptly at the radial internal pressure between 0.23 and 0.27 MPa (corresponded to regime of the second and third instant appeared during the expansion of the stent shown in Fig. 5), and was remained in an almost constant value after the radial internal pressure of 0.27 MPa (corresponded to regime of the fourth instant appeared during the expansion of the stent shown in Fig. 5) (Fig. 7). Generally, the stents with the closed unit cells connected to themselves or by a bar link structure (Palmaz-Schatz PS153, TenaxTM) had higher foreshortening values, whereas the stents with the opened unit cells connected by bend-shaped connector link structures (MAC Standard, MAC Plus, and Coroflex except to MAC Q23) or by an independent straight-line link structure (RX Ultra Multi-link) had lower foreshortening values (Table 2 and Fig. 7).

The dogboning values were positive for all balloon-stents, which indicates over-expansion of the distal points (i.e., POI No. 1–POI No. 4) of the stent, i.e., when the balloon-stent expanded, the distal points and the central point (POI No. 5) of the stent were spread out sequentially (Table 2 and Figs. 5 and 8). The maximum dogboning value for each stent was ranged from 19.4% for the MAC Plus stent to 64.3% for the Palmaz-Schatz PS153 stent (Table 2 and Fig. 8). For the POIs (POI No. 1–POI No. 4) of all stents, the dogboning was occurred suddenly at the radial internal

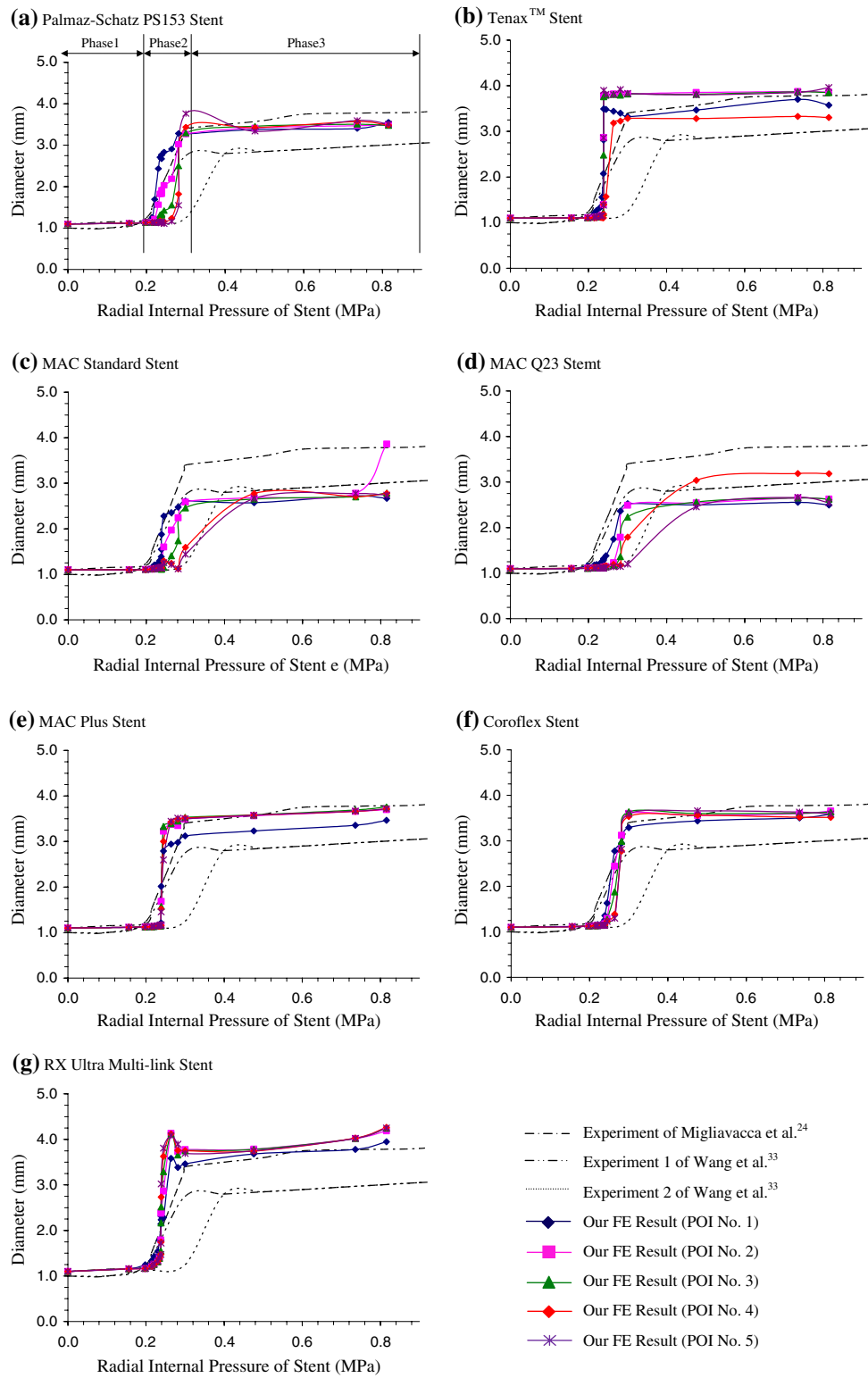


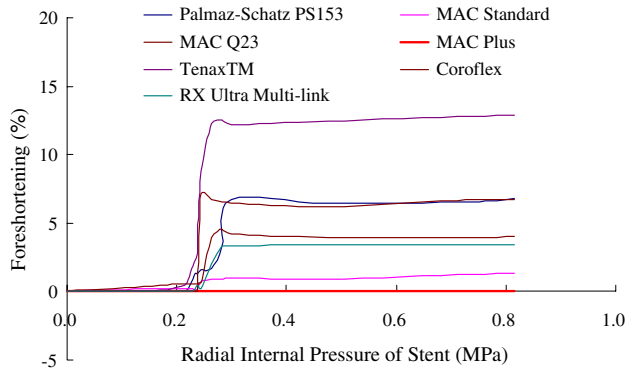
FIGURE 6. Pressure–diameter curve during the transient non-uniform balloon-stent expansion process obtained from the stents analyzed in the literature^{24,33} and the current study.

pressure between 0.23 and 0.27 MPa (corresponded to regime of the second and third instant appeared during the expansion of the stent shown in Fig. 5), and was

reduced and remained in an almost constant value after the radial internal pressure of 0.27 MPa (corresponded to regime of the fourth instant appeared

TABLE 2. Summarized quantitative results of the foreshortening and dogboning behaviors of the seven commercial stents.

Stent	Type of unit cell	Type of link structure	Maximum foreshortening (%)	Maximum dogboning (%)			
				POI No. 1	POI No. 2	POI No. 3	POI No. 4
Palmaz-Schatz PS153	Closed	No connector	6.8	64.3	51.1	41.3	15.7
Tenax™		Bar	12.9	46.4	47.9	46.7	32.5
MAC Standard	Opened	Bend-Shaped	1.3	59.0	46.8	33.9	26.9
MAC Q23			7.2	54.3	17.1	14.7	7.8
MAC Plus			0.0	19.4	42.1	33.3	23.7
Coroflex			4.5	48.0	37.8	21.3	8.8
RX Ultra Multi-link		Straight-Line	3.4	54.1	49.6	22.3	11.4

**FIGURE 7. Forshortening (%) along with radial internal pressure (MPa) during the transient non-uniform balloon-stent expansion process obtained from the stents analyzed in the current study.**

during the expansion of the stent shown in Fig. 5), similar to the foreshortening results (Fig. 8). Generally, for the POI No. 1, the stents with the closed unit cells connected to themselves (Palmaz-Schatz PS153) had higher dogboning value over 60%, whereas the stents with the closed unit cells connected by a bar link structure (Tenax™) or with the opened unit cells connected by bend-shaped connector link structures (MAC Standard, MAC Q23, MAC Plus, and Coroflex) or by an independent straight-line link structure (RX Ultra Multi-link) had lower dogboning values below 60% (Table 2 and Fig. 8). Here, a tendency for the results of the dogboning values for other POIs was similar to that for POI No. 1 (Table 2 and Fig. 8). Additionally, the results of the dogboning values showed that the stents with the closed unit cells connected to themselves (Palmaz-Schatz PS153) or with the opened unit cells connected by an independent straight-line link structure (RX Ultra Multi-link) had large differences among the dogboning values on the POIs (9.8–48.6% for Palmaz-Schatz PS153, 4.6–42.7% for RX Ultra Multi-link) (Table 2), whereas the stents the closed unit cells connected by a bar link structure (Tenax™) or with the opened unit cells connected by bend-shaped connector link structures (MAC

Standard, MAC Q23, and MAC Plus except to Coroflex) had relatively small differences among the dogboning values on the POIs (4.3–22.6% for Tenax™, 1.2–26.5% for MAC Standard, 7.0–27.4% for MAC Q23, 2.2–11.6% for MAC Plus, 10.2–39.2% for Coroflex) (Table 2). Here, from the magnitude of the difference, a degree of injury risk on the vascular wall induced by the dogboning can be expected. That is, if the difference is small, the stent is expanded evenly at the distal points of the stent, resulting in a reduction of restenosis risk.

DISCUSSIONS AND CONCLUSIONS

It is necessary to understand the relationship between the stent and the balloon, in order to identify an optimal stent design to minimize restenosis driven by foreshortening or dogboning. Carter *et al.*⁴ suggested that an injury to the adjacent arterial wall during stent deployment is an important determinant of in-stent neointimal formation, and short transitional edge protection balloon technology may be useful to reduce this kind of injury. Wang *et al.*³³ also discussed an importance of transient expansion process of balloon on the injury to the adjacent arterial wall during stent deployment, quoting Squire's finding that the manner in which stents are implanted was a critical determinant of the degree of injury. With all these points in mind, how to weaken or avoid these undesirable clinical outcomes is a key question that must be answered to reduce vascular injuries caused by foreshortening or dogboning. It is, therefore, especially important to pay attention to the design of the ends of the stent-balloon assembly with consideration of a realistic transient non-uniform balloon-stent expansion. This study may prove valuable as the first FE approach to investigate the design parameters capable of reducing restenosis induced by foreshortening or dogboning by considering a realistic transient non-uniform balloon-stent expansion.

There are basically two approaches that can be used to develop an optimal stent design by evaluating the

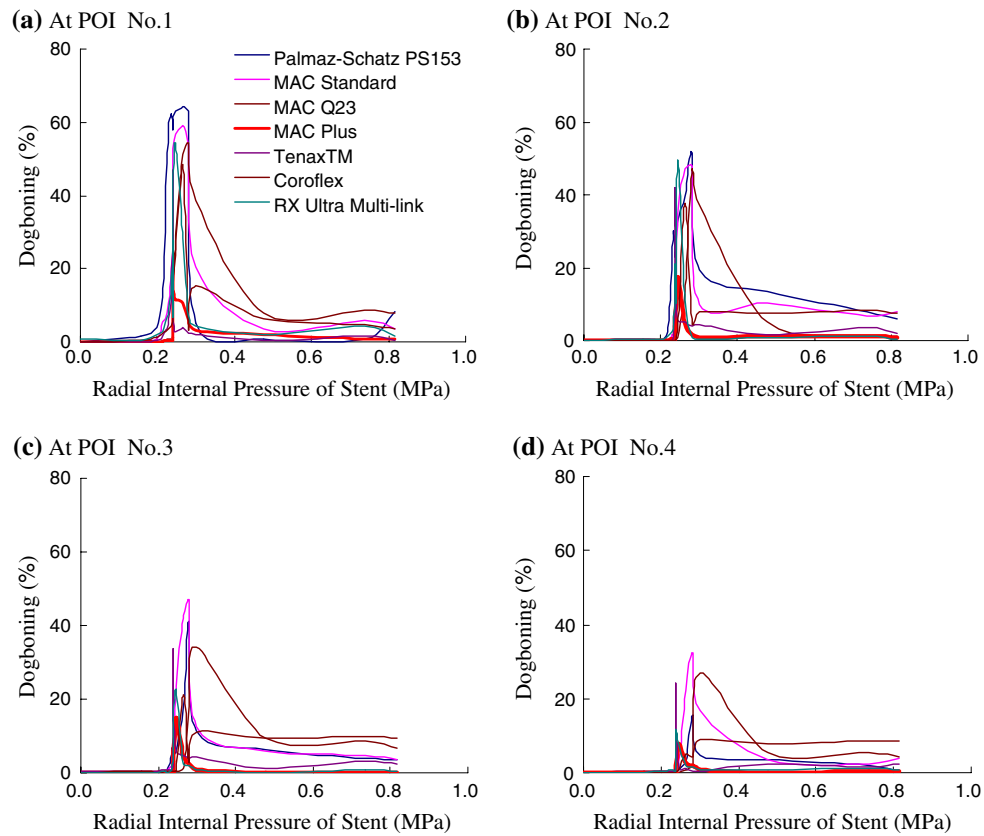


FIGURE 8. Dogboning (%) along with radial internal pressure (MPa) during the transient non-uniform balloon-stent expansion process obtained from the stents analyzed in the current study.

mechanical properties of various stents. The first approach involves directly measuring the mechanical properties of the stents by taking various balloon-stent configurations and expanding them to various diameters in normal or simulated diseased arteries, each with different characteristics. Due to the high cost, special construction, minute dimensions, dynamic characteristics of the deformation, and required animal tests, such a study would be prohibitively expensive and unachievable. The second approach involves computer analyses employing the FE method. In this way, simulations of various stents under different conditions can be carried out, and the results can be verified with experimental measurements of the specific stent behaviors. Adopting this approach reduces the costs substantially, thereby making a comparative study a viable proposition. Our FE simulations, particularly those of the transient non-uniform balloon-stent expansion, were validated favorably through comparison with experiment results reported in the literature and may be valuable for developing an optimal stent design while considering various balloon-stents configurations and different mechanical and physiological conditions.

Generally, the validation of FE models and simulations has been based on standard checks of the FE method, which should give a smooth load development, similar stress-strain plots of the structure against material property data, and smooth continuous contour lines across element boundaries. The FE models and simulations developed in the current study were validated integrally and practically by using these simple approaches as well as by comparing with experimental results from the literature. This may translate into more reasonable results for current and further applications of these FE models when studying an optimal stent design. An appropriate model of the arterial vessel and the atherosclerotic plaque, as well as correctly simulating their contact with the stent, is required to obtain fully accurate results for the mechanical behavior analysis and the optimal design of a stent. The lacks of inclusions of the blood vessel wall's mechanical characteristics such as compliance of the artery wall may create significant limitations in our current study. To date, FE models have focused on stent design parameters and not on restenosis.^{5-7,11,13,21,22,24,33} These studies, therefore, ignored the interaction between the stent and the blood vessel

wall. However, Rogers *et al.*²⁶ and Prendergast *et al.*²⁵ presented that considering the mechanical characteristics of the blood vessel wall in FE analysis is important because the interaction may influence a function of the stent. This fact indicates that considering the mechanical characteristics of blood vessel wall may be significant for the evaluations and the design analysis of the stents. The importance of the consideration of the mechanical characteristics of the blood vessel wall is, therefore, recently increased gradually in the evaluations and the design analysis of the stents.^{2,8,16} Holzapfel *et al.*¹⁶ presented the stent and stenotic artery FE models and analyzed stress states of the investigated artery during balloon-stent expansion. Berry *et al.*² used the FE analysis with the stent and artery FE models to understand better how the stent structure influences the stented blood vessel compliance and the circumferential stress at diastolic pressure. Chau *et al.*⁸ performed FE simulation of the slotted tube stent with the presence of plaque and artery by balloon expansion to investigate the expansion characteristics of the slotted tube stent. However, these studies did not analyze stent design parameters (i.e., foreshortening or dogboning) considering the actual transient non-uniform balloon-stent expansion to be simulated necessarily for investigation of the stent design parameters related to a primary cause of restenosis. They usually considered a uniform radial internal pressure with assumption based on the fact that stent is almost uniformly dilated and finally evenly expanded. The assumption is, however, only true away from the ends of stent and at the final stage of the stent expansion process, resulting in an inaccuracy in their results because the foreshortening or the dogboning is generally triggered at the early or middle stage of the stent expansion process as shown in Figs. 7 and 8. Although the current study addressed only the free transient non-uniform balloon-stent expansion without modeling the artery, our FE models and simulations were reasonable, at least qualitatively, when compared with experimental results identified from the literature, especially since this study focused on the potential design parameters capable of reducing restenosis driven by foreshortening or dogboning through identifying these characteristics in seven commercial stents. This study may, therefore, prove valuable as the first FE approach to investigate the design parameters capable of reducing restenosis induced by the foreshortening or the dogboning by considering the realistic transient non-uniform balloon-stent expansion as mentioned above.

The whole results for all stents analyzed in the current study showed that foreshortening and dogboning were generally higher in stents with closed unit cells connected by straight-line, and were generally lower in stents with opened unit cells connected by

bend-shaped link structures, in particular the MAC Plus stent. This finding indicates that using a stent composed of opened unit cells connected by bend-shaped link structures may prevent restenosis caused by foreshortening or dogboning. This finding is supported by Wang *et al.*³³ and Migliavacca *et al.*²¹ Wang *et al.*³³ reported that broadening the strut of the unit cells in the distal part of the stent may decrease dogboning, and the configuration of the link structure connecting the unit cells of the stent may determine the foreshortening characteristics of the stent. Wang *et al.*³³ also found that the absence of dogboning can decrease the foreshortening of the stent to a certain extent, but this effect is limited. Migliavacca *et al.*²¹ investigated the influence of the geometry of the stent on dogboning, foreshortening, and longitudinal recoiling by using FE methods and found that the thickness of the stent influenced its performance. By combining the current study with the findings of Wang *et al.*³³ and Migliavacca *et al.*²¹, we found that foreshortening and dogboning of stent-balloon systems were closely correlated with the configurations of the unit cells and the link structures as well as the distal geometry and morphology of the stent. Foreshortening and dogboning of the stent could be weakened both by using a stent composed of opened unit cells connected by the bend-shaped link structures and by controlling the distal stent strut width and thickness; the combination of these two methods will decrease the amount of foreshortening and dogboning.

Although this study provides a first look at the transient non-uniform balloon-stent expansion, there are the following limitations:

- (1) no consideration of the blood flow characteristics,
- (2) no consideration of the interaction between the stent and the artery, and
- (3) imperfect agreement between the stents used in the current study and in the literature^{11,24,33} for validation. This discrepancy was due to difficulties in obtaining the identical stents, balloons, and catheters that were used in the literature. However, the types of stents selected from the literature for the validation were similar to those used in the current study.

These limitations will be resolved and discussed in our ongoing studies incorporated with clinical tests.

ACKNOWLEDGMENT

This research was supported by the Generic Technology Development Program of the Korean Ministry of Commerce, Industry, and Energy.

REFERENCES

- ¹Albertini, C., and M. Montagnani. Dynamic uniaxial and biaxial stress-strain relationships for austenitic stainless steels. *Nucl. Eng. Des.* 57:107–123, 1980.
- ²Berry, J. L., et al. Hemodynamics and wall mechanics of a compliance matching stent: *in vitro* and *in vivo* analysis. *J. Vasc. Interv. Radiol.* 13:97–105, 2002.
- ³Bjarnason, H., et al. Collapse of a Palmaz stent in the subclavian vein. *Am. J. Roentgenol.* 160:1123–1124, 1993.
- ⁴Carter, A. J., et al. Experimental evaluation of a short transitional edge protection balloon for intracoronary stent deployment. *Catheter. Cardiovasc. Interv.* 51:112–119, 2000.
- ⁵Chua, S. N. D., et al. Finite-element simulation of stent expansion. *J. Mater. Process. Technol.* 120:335–340, 2002.
- ⁶Chua, S. N. D., et al. Finite element simulation of stent and balloon interaction. *J. Mater. Process. Technol.* 143–144:591–597, 2003.
- ⁷Chua, S. N. D., et al. Effects of varying slotted tube (stent) geometry on its expansion behaviour using finite element method. *J. Mater. Process. Technol.* 155–156:1764–1771, 2004.
- ⁸Chua, S. N. D., et al. Finite element simulation of slotted tube (stent) with the presence of plaque and artery by balloon expansion. *J. Mater. Process. Technol.* 155–156:1772–1779, 2004.
- ⁹Dangas, G., and V. Fuster. Management of restenosis after coronary intervention. *Am. Heart J.* 132:428–436, 1996.
- ¹⁰Dotter, C. T. Transluminally placed coil spring end arterial tube graft, long-term patency in canine popliteal artery. *Invest. Radiol.* 4:329–332, 1969.
- ¹¹Dumoulin, C., and B. Cochelin. Mechanical behavior modeling of balloon-expandable stents. *J. Biomech.* 33:1461–1470, 2000.
- ¹²Erbel, R., et al. Coronary-artery stenting compared with balloon angioplasty for restenosis after initial balloon angioplasty. *N. Engl. J. Med.* 339:1672–1678, 1998.
- ¹³Etave, F., et al. Mechanical properties of coronary stents determined by using finite element analysis. *J. Biomech.* 34:1065–1075, 2001.
- ¹⁴Fischman, D. L., et al. A randomized comparison of coronary-stent placement and balloon angioplasty in the treatment of coronary artery disease. *N. Engl. J. Med.* 331:496–501, 1994.
- ¹⁵Freitag, L., et al. Theoretical and experimental basis for development of dynamic airway stent. *Eur. Respir. J.* 7:2038–2045, 1994.
- ¹⁶Holzapfel, G., et al. A layer-specific three-dimensional model for the simulation of balloon angioplasty using magnetic resonance imaging and mechanical testing. *Ann. Biomed. Eng.* 30:753–767, 2002.
- ¹⁷Kandzari, D. E., et al. Coronary artery stents: evaluating new designs for contemporary percutaneous intervention. *Catheter. Cardiovasc. Interv.* 56:562–576, 2002.
- ¹⁸Kastrati, A., et al. Restenosis after coronary placement of various stent types. *Am. J. Cardiol.* 87:34–39, 2001.
- ¹⁹Lohavanichbutr, K., et al. Mechanisms, management, and outcome of failure of delivery of coronary stents. *Am. J. Cardiol.* 83:779–781, 1999.
- ²⁰MatWeb. Dupont Fusabond E MB100D High Density Polyethylene, Available at <http://www.matweb.com/search/SpecificMaterial.asp?bassnum=PDUPM015>. MatWeb Material Property Data, 2006.
- ²¹Migliavacca, F., et al. Mechanical behavior of coronary stents investigated through the finite element method. *J. Biomech.* 35:803–811, 2002.
- ²²Migliavacca, F., et al. Stainless and shape memory alloy coronary stents: a computational study on the interaction with the vascular wall. *Biomech. Model. Mechanobiol.* 2:205–217, 2004.
- ²³Migliavacca, F., et al. A predictive study of the mechanical behaviour of coronary stents by computer modelling. *Med. Eng. Phys.* 27:13–18, 2004.
- ²⁴Migliavacca, F., et al. A predictive study of the mechanical behavior of coronary stents by computer modeling. *Med. Eng. Phys.* 27:13–18, 2005.
- ²⁵Prendergast, P. J., et al. Analysis of prolapse in cardiovascular stents: a constitutive equation for vascular tissue and finite-element modelling. *J. Biomech. Eng.* 125:692–699, 2003.
- ²⁶Rogers, C., et al. Balloon artery interactions during stent placement. A finite element analysis approach to pressure, compliance, and stent design as contributors to vascular injury. *Circ. Res.* 84:378–383, 1999.
- ²⁷Rosenfield, K., et al. Restenosis of endovascular stents from stent compression. *J. Am. Coll. Cardiol.* 29:328–338, 1997.
- ²⁸Schwartz, R. S. Pathophysiology of restenosis: interaction of thrombosis, hyperplasia, and/or remodeling. *Am. J. Cardiol.* 81:14E–17E, 1998.
- ²⁹Serruys, P. W., et al. A comparison of balloon-expandable stent implantation with balloon angioplasty in patients with coronary artery disease. *N. Engl. J. Med.* 331:489–495, 1994.
- ³⁰Stefanidis, I. K., et al. Development in intracoronary stents. *Hellenic J. Cardiol.* 43:63–67, 2002.
- ³¹Suwaidi, A. I., et al. Coronary artery stents. *J. Am. Med. Assoc.* 284:1828–1836, 2000.
- ³²Timmins, L. H., et al. Stented artery biomechanics and device design optimization. *Med. Biol. Eng. Comput.* 45:505–513, 2007.
- ³³Wang, W. Q., et al. Analysis of the transient expansion behavior and design optimization of coronary stents by finite element method. *J. Biomech.* 39:21–32, 2006.
- ³⁴Wong, P., et al. Migration of the AVE micro coronary stent. *Catheter. Cardiovasc. Diagn.* 38:267–27, 1996.